

1 Article

# 2 Preparation and characterization of an electrospun 3 PLA-cyclodextrins composite for simultaneous high- 4 efficiency PM and VOC removal

5 Silvia Palmieri <sup>1\*</sup>, Mattia Pierpaoli <sup>2\*</sup>, Luca Riderelli <sup>3</sup>, Sheng Qi <sup>4</sup> and Maria Letizia Ruello <sup>1,\*</sup>

6 <sup>1</sup> Department of Materials, Environmental Sciences and Urban Planning-(SIMAU), Università Politecnica  
7 delle Marche, Ancona, Italy; s.palmieri@pm.univpm.it (SP), m.l.ruello@univpm.it (MLR)

8 <sup>2</sup> Department of Metrology and Optoelectronics, Faculty of Electronics, Telecommunication and Informatics,  
9 Gdańsk University of Technology, Gdańsk, Poland; mattia.pierpaoli@pg.edu.pl

10 <sup>3</sup> Professional Engineer, Via Bartolini 13/A, 60027 Osimo, Ancona, Italy; lucariderelli@gmail.com

11 <sup>4</sup> School of Pharmacy, University of East Anglia, Norwich Research Park, Norwich, UK NR4 7TJ

12 \* Correspondence: (SP) s.palmieri@pm.univpm.it; (MLR) m.l.ruello@univpm.it; (MP)  
13 mattia.pierpaoli@pg.edu.pl;

14 Received: date; Accepted: date; Published: date

15 **Abstract:** Electrospinning is known to be a facile and effective technique to fabricate fibres of a  
16 controlled diameter-distribution. Among a multitude of polymers available for the purpose, the  
17 attention should be addressed to the environmentally compatible ones, with a special focus on  
18 sustainability. Polylactic acid (PLA) is a widespread, non-toxic, originated from renewable sources,  
19 polymer and it can degrade into innocuous products. While the production of fibrous membranes  
20 is attractive for airborne particles filtration applications, their impact on the removal of gaseous  
21 compounds is generally neglected. In this study, electrospun PLA-based nanofibers were  
22 functionalized with cyclodextrins, because of their characteristic hydrophobic central cavity and a  
23 hydrophilic outer surface, in order to provide adsorptive properties to the composite. The aim of  
24 this work is to investigate a hybrid composite, from renewable sources, for the combined filtration  
25 of particulate matter (PM) and adsorption of volatile organic compounds (VOCs). Results show how  
26 their inclusion into the polymer strongly affects the fibre morphology, while their attachment onto  
27 the fibre surface only positively affects the filtration efficiency.

28 **Keywords:** Polylactic Acid; electrospinning; nanofibers; air filtration

---

## 30 1. Introduction

31 Air filtration is the most effective and widespread method to remove particulate matters (PM)  
32 from the air stream. Air filter material and morphology play a major role in the process efficiency and  
33 sustainability. Electrospinning is a versatile method commonly used to manufacture polymer  
34 nanofiber[1].

35 The concept of green electrospinning has been introduced with the aim of reducing the toxicity and  
36 environmental problem related to the use of potentially hazardous-organic solvents for the  
37 electrospinning of natural or synthetic polymers [2]. While this aspect is of primary importance in  
38 regenerative medicine, in which the absence of impurity is compulsory, when the electrospun fibre  
39 mat is used in much larger extends for air filtration applications, the focus should be addressed to  
40 the polymer type as well, favouring polymer from renewable sources, easily disposable, having a low  
41 environmental impact. Since indoor air quality has become not only an issue but also a need, due to  
42 the risks people are exposed to and in connection with the amount of time spent in confined  
43 environment, both at work and home [3]. In addition to common pollutants of outdoor air, it must

44 be considered other unusual sources like furniture, copiers, and air fresheners, and so on. Also,  
 45 people themselves are a source of potentially harmful agents i.e. spread as indoor bioaerosol.

46 Electrospinning of functional polymeric nanofibers has attracted considerable attention in the past  
 47 decade due to the simplicity of the process and the enhanced properties associated with the size of  
 48 the fibres [4–6]. One potential application for electrospun nanofibers is in the field of filtration where  
 49 the nanowebs can provide separation of tiny particles due to the different interception mechanism.

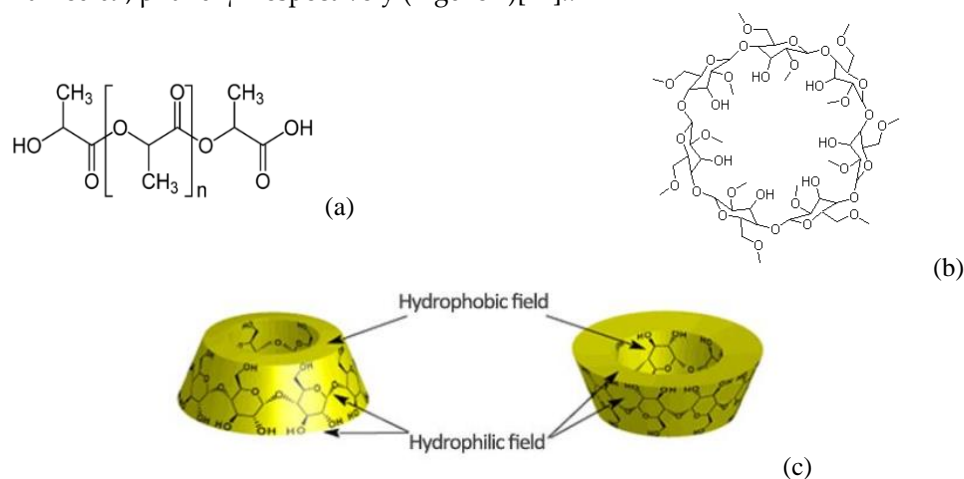
50 PLA is a thermoplastic aliphatic polyester derived from renewable resources, so it has been  
 51 chosen for its environmentally friendly properties as its biodegradability.

52 The fabrication of PLA electrospun nanofibers has been widely investigated by many authors because  
 53 of the great availability, the production from renewable sources, the non-toxicity, and the known  
 54 biodegradability[7–9]

55 Casasola and co-workers [10] investigated the effect of different solvents on the fibre morphology. In  
 56 particular, they found that the acetone-based binary solvent system was the most effective to produce  
 57 electrospinnable nanofibers.

58 In the study of Wang et al. [11], porous bead-on-string poly(lactic acid) (PLA) nanofibrous  
 59 membranes (NMs) were fabricated to investigate the filtration performance by measuring the  
 60 penetration of sodium chloride (NaCl) aerosol particles. Without further modification, a high  
 61 filtration efficiency was obtained, by controlling the solvent solution.

62 Cyclodextrins (CDs) are conical, truncated macrocycles, consist of six, seven, and eight  $\alpha$ -d-glucose  
 63 units, and named  $\alpha$ -,  $\beta$ - and  $\gamma$ - respectively (Figure 1)[12]..



64 **Figure 1.** a) PLA chemical structure; (b) CyD chemical structure; (c) representation of CyD  
 65 structure.

66 They are environmentally friendly and deserve attention for their valuable properties thanks to their  
 67 chemical structure. In fact, they are commonly applied in different fields: from pharmaceutical  
 68 carriers [12–14] to the use as nano-sponges in water treatments [13,15].. Cyclodextrins can form  
 69 complexes of inclusion with numerous poorly soluble molecules, this is the reason why they are  
 70 commonly used in pharmaceutical chemistry as carriers. Hydrophobic molecules are maintained in  
 71 the cavity of the cyclodextrin with the outer surface of the complex maintaining its hydrophilic  
 72 characteristics [12,16]. Wen and colleagues [17] incorporated cinnamon essential oil/beta-  
 73 cyclodextrin into PLA nanofilm to give better antimicrobial activity compared to conventional  
 74 nanofilm, prolong the shelf life of food, as an active food packaging. Similarly, in the works of Aytac  
 75 et al.[18], beta-cyclodextrin is used for the stabilization of active compounds in the production of  
 76 functional electrospun PLA nanofibers incorporating naturally occurring antioxidant compound [18].  
 77 Taking advantages of their molecular structure to block lipophilic molecules, such as volatile organic  
 78 compounds (VOCs), another use for cyclodextrins has been proposed [20,21] for air pollution control  
 79 applications. While cyclodextrins have already been used for the removal of organic pollutants in  
 80 wastewater [15,21,22], they have not been used in much lesser extends for air treatments and removal  
 81 of PMs and VOCs.

82 In this study, for the first time, an electrospun PLA/cyclodextrin composite has been produced  
83 and characterized for the joint filtration of particulate matter (PM) and enhanced adsorption of VOCs.  
84 The electrospun nanocomposite exhibits not only excellent PM filtration efficiency, but the presence  
85 of CyD provides to the composite material a two-fold improved adsorption ability measured in terms  
86 of toluene removal.

## 87 2. Materials and Methods

### 88 2.1 Material

89 Dichloromethane (DCM) and N,N-Dimethylformamide (DMF) of analytical grade were  
90 purchased from Sigma-Aldrich. PLA has been used to prepare a polymeric solution of 8% w/V  
91 solubilized in DCM/DMF (80:20). The electrospinning setup consists of a house-made syringe pump,  
92 which needle is connected to the high potential (16kV). The flow rate was 0.5 ml/h and the  
93 needle/collector distance equal to 10cm. Nanofibers are electrospun over a PLA-based 3D printed  
94 support, placed on a grounded aluminium foil (See supplementary materials).

95 All the prepared composites were electrospun over 3D-printed support (1mm thick) with large  
96 voids (60% fill). Pictures of the substrate and 3d printing parameters are reported in the supporting  
97 materials. Both support and nanofibers produced with electrospinning technique are made by the  
98 same polymer to improve the affinity, permitting a better adhesion between them [23]. [12,19] In this  
99 study B-methyl-cyclodextrins (Carbosynth) have been also used either in association with fibers as  
100 such (in powder) or solubilized in methanol (Sigma-Aldrich) and electrospun. Cyclodextrins were  
101 both incorporated in the PLA solution, both dispersed on the PLA surface. Three different  
102 configurations were studied: a) PLA solubilized in the solvent and then electrospun (PLA); b) a three  
103 levels configuration where a layer of cyclodextrins in powder was placed in the middle of a bi-layer  
104 of electrospun PLA (PLA/CyD); c) Cyclodextrins were solubilized in few droplets of methanol and  
105 added in the same solution of PLA then electrospun (PLA+CyD).

### 106 2.2. Characterization

107 All the specimens have been analyzed with a ZEISS Scanning electron microscope for the  
108 characterization of the morphological aspect and to evaluate the interaction between PLA fibres and  
109 CyD.

110 The samples were analyzed by using a Perkin-Elmer Spectrum GX1 spectrometer (PerkinElmer,  
111 Inc, Waltham, MA, USA) equipped with U-ATR accessory for the analysis of solid samples in  
112 reflectance mode. On each sample, 5 spectra were acquired in the range between 4000-500  $\text{cm}^{-1}$ , with  
113 a spectral resolution of 4  $\text{cm}^{-1}$  and recording 64 scans. A background adsorption spectrum was  
114 recorded before each acquisition. Raw FTIR spectra were converted in absorbance, interpolated in  
115 the 1800-500  $\text{cm}^{-1}$  spectral range and vector normalized in the same interval. An automatic baseline  
116 correction algorithm was used in all spectra to avoid errors due to baseline shifts. Atmospheric  
117 compensation was also performed. The average absorbance spectra of all samples were also  
118 calculated, and they were fitted in the 1800-800  $\text{cm}^{-1}$  upon two-points baseline correction and vector  
119 normalization (Grams AI 9.1 software, Galactic Industries, Inc., Salem, NH). A Gaussian algorithm  
120 was adopted. For each underlying band, the positions in terms of wavenumbers, height and  
121 integrated area were calculated. Spectrum 5.3.1 (Perkin-Elmer) was used as the operating software.

### 122 2.3. PM generation and efficiency tests

123 In the filtration efficiency tests, PM particles were generated by burning incense in an 82 l box.  
124 The smoke PM particles have a wide size distribution from <300 nm to 4  $\mu\text{m}$ , with the majority of  
125 particles being <1  $\mu\text{m}$ . The so-generated particle stream was controlled by dilution with air. PM  
126 particle number concentration was measured with a GRIMM 1.108 particle counter and the removal  
127 efficiency was calculated by comparing the number concentration before and after filtration, while  
128 the pressure drop in the filter medium was measured by a differential pressure meter (Honeywell

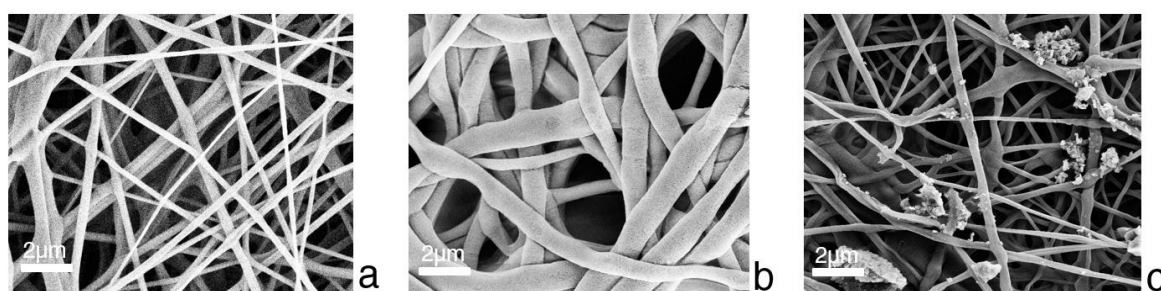
129 160 PC). The wind velocity, measured in absence of the filter with a hot-wire anemometer, was equal  
 130 to  $1.4 \text{ m s}^{-1}$ .

131 VOC removal tests were performed in the same box environments, with the injection of  $100 \mu\text{l}$   
 132 Toluene, and the test started when its full vaporization occurred. VOC concentration was measured  
 133 with a ppbRAE 3000 with 1-min sample time, and the VOC removal efficiency was calculated,  
 134 likewise for PM, by comparing the number concentration before and after filtration. All the tests were  
 135 performed at the temperature of  $27 \pm 2^\circ\text{C}$  and RH equal to  $50 \pm 10\%$ .

136 **3. Results**

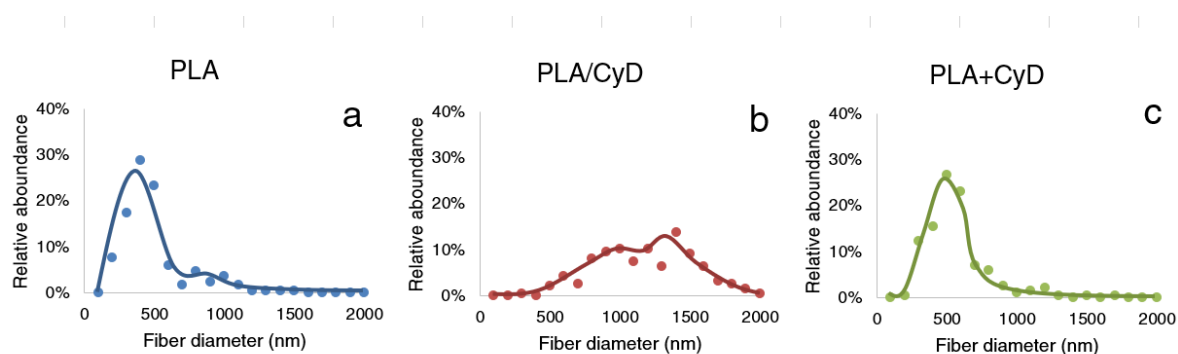
137 *3.1. Electrospun nanofiber morphology*

138 Figure 2 reports SEM pictures of the three reference filter composites, with only PLA (Figure 2a),  
 139 with the addition of CyD in bulk solution (Figure 2b) and over the PLA fibre (Figure 2c). The median  
 140 diameters of the PLA-based fibres composites electrospun from the solutions were determined to be  
 141 350, 990, and 530 nm, respectively (Figure 3.)



142

143 **Figure 2.** SEM pictures of (a) PLA, (b) PLA/CyD and (c) PLA+CyD electrospun nanofibers.



144

145 **Figure 3.** Fiber diameter distribution for (a) PLA, (b) PLA/CyD and (c) PLA+CyD  
 146 electrospun nanofibers.

147 The Fibrous filter pressure drops were measured at low face velocity. Pressure drop and outlet  
 148 air velocity, as a function of the fibre type and fibre loading values, have been reported in Table 1.

149 **Table 1.** Composition and characterization of the electrospun filter media.

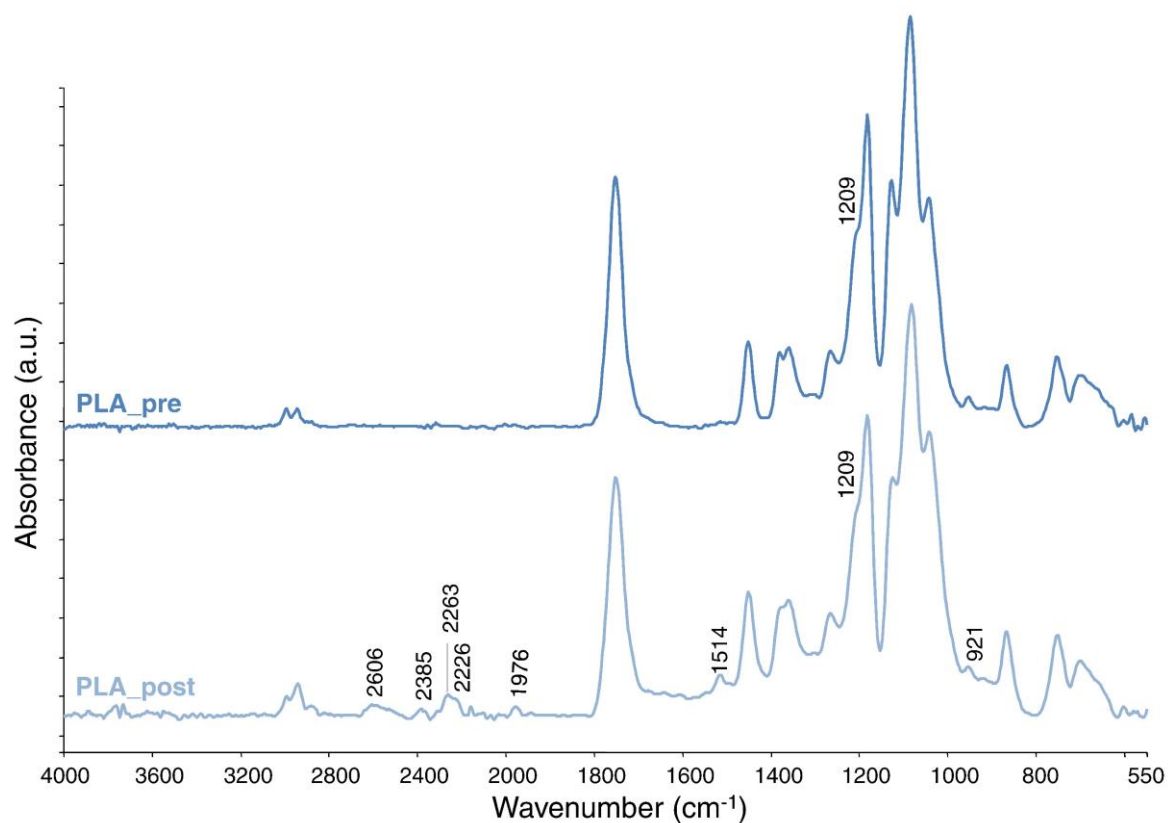
Filter	solution		CyD	$v_{\text{outlet}}$ (m/s)	$\Delta P$ (Pa)	Filter loading ( $\text{mg}/\text{cm}^2$ )
	PLA	CyD				
PLA	100%	0	-	0.25	24.4	1.43
PLA/CyD	98.5%	1.5%	-	0.41	33.9	2.47
PLA+CyD	100%	-	1.5%	0.24	29.9	4.05

150

151 Starting with these data, analyses on images were carried out to find out correlations with  
152 dimensions and morphology of the fibres. Observing the three filters (Figure 2), cyclodextrins  
153 influence the result of electrospinning and the overall measured pressure drop (Table 1,  $\Delta P$  24.4, 33.9,  
154 and 29.9 respectively). Filters PLA/CyD show apparently more bulky fibres (Table 1, Filter loading  
155 (mg/cm<sup>2</sup>), 1.43, 2.47, and 4.05) fibres than the ones of PLA and PLA+CyD filters. This comparison  
156 justifies a higher drop pressure for this filter (33.9 Pa). Furthermore, crossing fibres enhance thickness  
157 determining a probably augmented capacity of sieving phenomena. PLA mix differentiates itself  
158 from PLA/CyD and PLA+CyD only for the addition of CyD.

### 159 3.2. FTIR Spectroscopy

160 FTIR spectroscopy was used to determine the interaction between both PLA and CyD and the  
161 composite and pollutants[24]. Obviously, due to a large number of functional groups present due not  
162 only to the enormous variability of the compounds present in the polluting source used for the tests  
163 but also to the polymeric ones of the filter, it is not possible to identify with certainty the filtered  
164 molecules. It is instead possible to determine by the difference the presence or absence of pollutants.  
165 In this regard, it was necessary to outline a spectroscopic profile of the materials used to make the  
166 filter itself, to also study the interaction between the polymer and the CyDs. The enormous variety of  
167 compounds present in the polluting source does not always and unequivocally allow to have the  
168 same peaks, so it is necessary to search for the traces of pollutant by evaluating the shifts and all the  
169 variations between the different peaks. Figure 4 reports a comparison between the untested and the  
170 tested PLA filter (without CyDs). The spectra of the pristine filter show the main peaks attributable  
171 to the PLA: at 2997-2944cm<sup>-1</sup> there are the symmetrical and the asymmetrical stretching of CH<sub>2</sub> and  
172 CH<sub>3</sub>; the characteristic peak of a carbonyl group is at 1753 cm<sup>-1</sup>; at 1453 cm<sup>-1</sup> there is the methyl in  $\alpha$   
173 position respect to the carbonyl group and in the region of 1380-1000cm<sup>-1</sup> the bending signals of CH<sub>2</sub>  
174 and CH<sub>3</sub>.



175

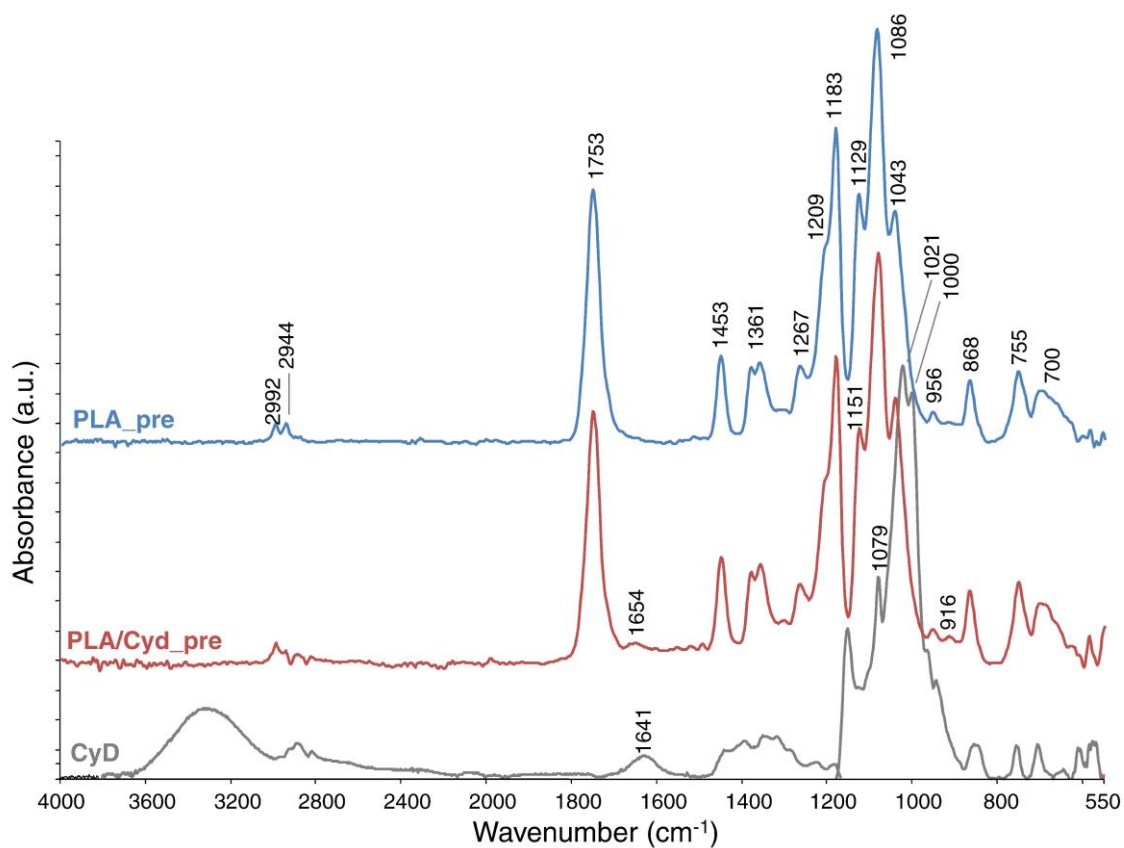
176

Figure 4. FTIR spectra of tested and untested PLA filters.

177 In the other spectra, the different peaks caused by the interaction of the polymer with pollutants  
178 can be easily individuated: at 1644, 1541, 1514, 1301  $\text{cm}^{-1}$  and 953  $\text{cm}^{-1}$ . Confronting the peak of the  
179 carbonyl group at 1753  $\text{cm}^{-1}$  of the no tested filter with the same peak of the other samples reports a  
180 shift caused by the interaction between the polymer and the pollutant. It is possible to suppose the  
181 presence of nitro groups, reported by the peaks in the range of 1541 $\text{cm}^{-1}$  and 1514  $\text{cm}^{-1}$ ; the presence  
182 of aldehydes because of the shift at 1754  $\text{cm}^{-1}$  and the peak at 1644 $\text{cm}^{-1}$ ; and a carbon-nitrogen bond,  
183 due to the presence of a peak at 1301 $\text{cm}^{-1}$ .

184 The peak at 1514 $\text{cm}^{-1}$  is very sharp respect to the other spectres, it is reasonable to assume that  
185 this is due to the concentration of pollutant adsorbed. A peak at 1514 $\text{cm}^{-1}$  can be attributed or to a NO  
186 or a CN group. Moreover, it presents a series of peaks at 2601, 2385, 2263 and 1976 $\text{cm}^{-1}$ . Usually, in  
187 this range, there are signals from inorganic contaminants as, for example, thiocyanate. Considering  
188 the CN at 1514 $\text{cm}^{-1}$  at the level of bands' ratio, the signal of the triple bonds is present at 2200 $\text{cm}^{-1}$ ; the  
189 -SH group is at 2600  $\text{cm}^{-1}$  and the signal of SCN is at 2100  $\text{cm}^{-1}$ . The peak at 1209 $\text{cm}^{-1}$  is different in  
190 terms of height, therefore the concentration of the respective group increases after the filtration, so a  
191 pollutant containing the same group is attached to the filter. Lastly, at 921  $\text{cm}^{-1}$  a new peak appears,  
192 which was absent in the pristine filter, so it is may be relative to the deposited pollutant.

193 For what concerns the filters made with the addition of cyclodextrins (PLA/CyD and PLA+CyD),  
194 it was important to determinate the possible interaction between the polymer and the CyD molecules,  
195 because during the electrospinning process these two compounds could interact causing the presence  
196 of new peaks independent from the wavelengths of the single compounds. It was necessary to  
197 determine the shifts and the new peaks on a no tested filter, not only to have a reference standard for  
198 the identification of the pollutant, but also to estimate the level of the bond between the two  
199 compounds. In Figure 5 is reported the spectra of the filter untested, made by adding CyD not only  
200 in the between of two layers of the polymer (PLA+CyD), but also in the polymer solution (PLA/CyD).  
201 Analysing this spectrum, it is immediately notable the absence of the characteristic peak of the  
202 hydroxylic group at 3400 $\text{cm}^{-1}$ , because a large quantity of these groups is bonded with PLA in  
203 hydrogen bonds; but the peak at 1654 $\text{cm}^{-1}$  indicates that there are still some free. All the values at  
204 1000, 1021, 1077 and 1151  $\text{cm}^{-1}$  are shifted to 1040, 1082, 1124 and 1182  $\text{cm}^{-1}$  because of the hydrogen  
205 bonds between the two compounds. Also, the peak at 850 $\text{cm}^{-1}$ , typical of C-C bond, is shifted to 916  
206  $\text{cm}^{-1}$ . The shift of the signal can be caused not only by the formation of new bonds but also by the sum  
207 of two different signals in the same region.



208

209

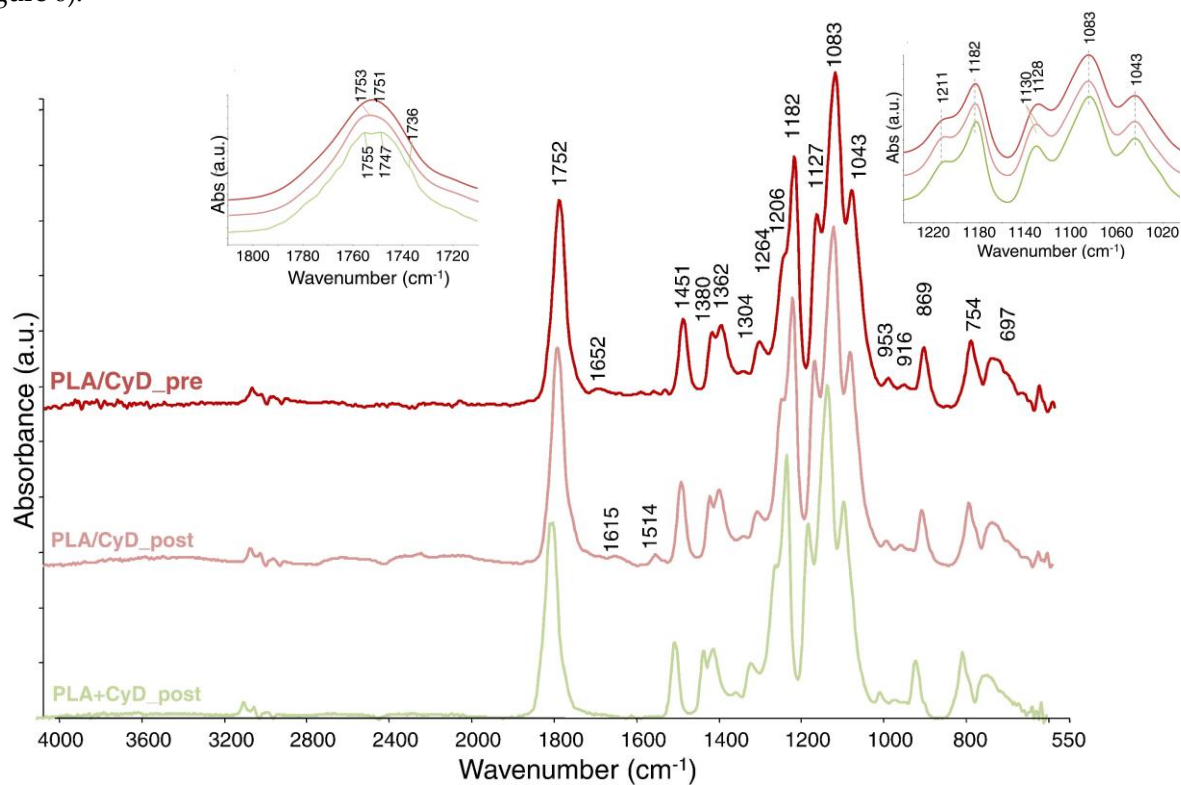
**Figure 5.** Typical spectra of the filter containing PLA and CyDs.

210

After the reference spectra for the filters containing CyD, also the tested spectra were examined

211

(Figure 6).



212

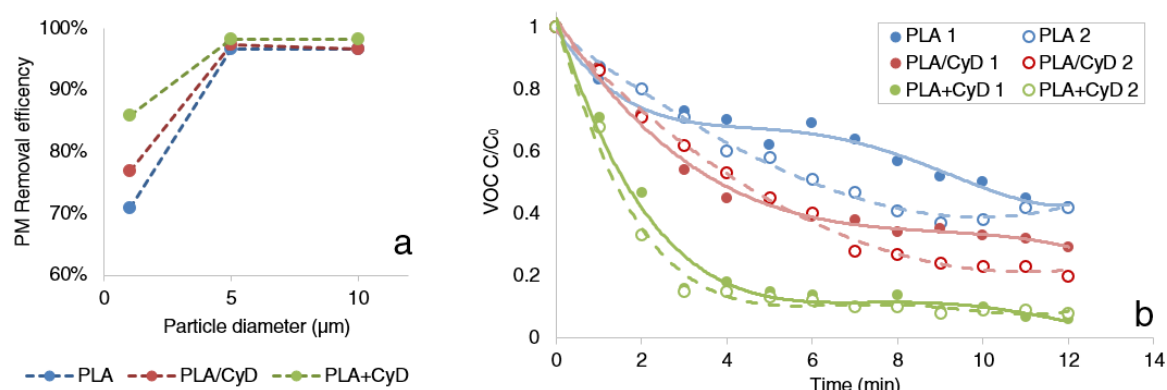
213

**Figure 6.** Comparison between all the filters containing cyclodextrins.

214 In these samples the presence of contaminates is represented by two main behaviours: the most  
 215 important is the split of the carbonyl peak and its slightly shift; the other change is the shift of all the  
 216 characteristic bands in the range from  $1220\text{ cm}^{-1}$  to  $1000\text{ cm}^{-1}$ . The split of the carbonyl group can  
 217 indicate the presence of another molecule with a similar configuration (for instance it can be an  
 218 aldehyde or a ketone). Moreover, these kinds of pollutants may cause also the shoulder at  $1736\text{ cm}^{-1}$ .  
 219 Other particular peaks are present at  $3377\text{ cm}^{-1}$  for PLA/CyD: the peak at  $3377\text{ cm}^{-1}$  can be attributed to  
 220 a compound with NH group, seeing as there are also peaks at  $1615$  and  $1514\text{ cm}^{-1}$ , which usually  
 221 indicate the presence of  $\text{NH}_2$  and of a carbon bonded to nitrogen. The series of peaks in the range  
 222 from  $870$  to  $700\text{ cm}^{-1}$  are typical of CH groups: in these cases, they are different from the reference  
 223 because of their shape and their shift, indicating the presence of another compound different from  
 224 Cyclodextrins or PLA.

### 225 3.3. PM and VOC removal tests

226 The  $\text{PM}_{10}$ ,  $\text{PM}_{2.5}$  and  $\text{PM}_{10}$  removal by different fibrous filters is shown in Figure 7(a). From the  
 227 PM efficiency removal comparison, it is possible to observe that the PLA+CyD has the highest  
 228 removal of both smaller particles, while all the different samples exhibit an efficiency higher than  
 229 97% for particles having diameter greater than  $2.5\text{ }\mu\text{m}$ .



230

231 **Figure 7.** (a) PM removal efficiency and (b) normalized VOC concentration versus time by  
 232 the different fibrous filters.

233 The characteristic conical configuration of cyclodextrins [12] is suitable for the formation of  
 234 complexes of inclusion through non-covalent interactions: in fact, hydrophobic molecules are  
 235 maintained in the cavity, blocking their passage through the filter.

236 This mechanism of filtration should be added, according to classical filtration theory, to the other  
 237 five mechanism effects to catch particles (interception, inertial, diffusion, gravity, and static electricity  
 238 effect) [25] to catch also other smaller molecules as VOCs. In this way, CyD plays a role both in  
 239 affecting the fibre morphology, resulting in thicker fibres and reduced cavities, and, actively, as  
 240 surface centres for the capture of PM and VOCs, due to their dual hydrophilic/hydrophobic nature.  
 241 The presence of CyD molecules at the surface of the fibres has a large influence on the molecular  
 242 filtration capability [26]. The presence of more CyDs on the surface of the fibres implies a higher  
 243 availability of sites for the bond with the pollutants, so it is reasonable to assume that higher  
 244 concentration of CyDs are beneficial for the overall filtration efficiency. Nevertheless, the superficial  
 245 availability of adsorption centres will affect also the blocking capacity of PMs and the resulting  
 246 pressure drop. For all these reasons, the amount of CyDs must be enough to be bonded to the polymer  
 247 and sufficient to have the possibility to create hydrogen bond with the pollutants.

248 During the electrospinning, CyD molecules could phase separate from PLA matrix and formed  
 249 heterogeneous dispersion during solvent evaporation in the electrospinning process: this is likely  
 250 because CyD has a hydrophilic characteristic and PLA is a hydrophobic polymer [26]. A heterogenic  
 251 solution may cause a not homogeneous presence of CyDs on the fibre surface, causing a not  
 252 homogenous filter.

253 VOCs removal is shown in Figure 7(b). In this graph, it is possible to compare the three different  
 254 tested filters in two subsequent situations. These tests were conducted injecting Toluene in the box.  
 255 The first curve is about the behaviour with 100  $\mu$ l of Toluene (in Figure 7(b) labelled with 1). After  
 256 about 30 minutes and as curves reach a plateau or their background concentration, the second  
 257 injection of Toluene was carried out (20  $\mu$ l). This second injection (in Figure 7(b) labelled with 2) is  
 258 sufficient to obtain an initial concentration of Toluene comparable to the first one. The purpose of this  
 259 method consists in investigating repeatability of tests and in the first evaluation of the durability of  
 260 filters. As it was expected, filters with cyclodextrins allow quicker removal of VOCs, referred to PLA  
 261 only fibres. Besides, it can be observed that the two normalized curves are almost overlapped,  
 262 highlighting a factual constant behaviour, for two subsequent tests at high concentration at least.

263 The presence of cyclodextrins in filters points out an increased capacity in the removal of VOCs.  
 264 This condition suggests that VOCs removal tests highlight the contribution of the CyD on adsorption.  
 265 Thus, the CyD can empower the removal of VOCs in two different ways. It is probable that in  
 266 PLA/CyD filters VOCs are removed when CyD have their hole available. In PLA+CyD filters, VOCs  
 267 are removed when they collide with CyD powder with an enhanced capacity of removal because of  
 268 entire exposure to air, with a higher number of available sites.

269 A non-exhaustive comparison of the obtained results with the one reported in the literature is  
 270 reported in Table 2.

271 *Table 2 – Comparison of the obtained filtration results with the one reported in the literature*

Electrospun Polymer	Efficiency	Comments	Ref
PLA	99.997% (165.3 Pa)	Small fibre diameter and the presence of additional mesopores on the beads were conducive to the capture and adsorption of particulates.	[11]
PLA/TiO <sub>2</sub>	99.996% (128.7 Pa)	Relative humidity of 45% and face velocity of 5.3 cm/s and a high antibacterial activity of 99.5%	[27]
PLA/CNPs	98.99% (147.60 Pa)	Air flow rate of 14 cm/s. PLA/chitosan fibres show a highly porous structure	[28]
PVA/CNCs	99.1% (91 Pa)	Tests with PM2.5 and airflow velocity of 0.2 m/s	[29]
Hierarchical structured nano-sized/porous PLA	99.999% (93.3 Pa)	PLA-N/PLA-P double-layer structured membrane with a mass ratio of 1/5. Face velocity of 5.3 cm/s	[30]
PAN	>99% (27 Pa)	Nanobeads are useful for reducing the packing density and the pressure drop through the filter. Ultrafine nanofibers guarantee the PM removal efficiency. Airflow rate of 4.2 cm/s	[31]
PLA/CyD	> 98% (30Pa)		<i>This study</i>

272 DMAC: dimethylacetamide; CNPs: Chitosan nanoparticles; CNCs: cellulose nanocrystals

#### 273 4. Conclusions

274 The addition of CyD both in bulk and powder determines an increase of removal efficiency of  
 275 VOCs and PM1 size fraction, due to two different effects: the CyD in bulk affect the PLA fibres  
 276 morphology, while the superficially deposited CyD directly affect the removal of the VOC. Efficiency  
 277 tests highlight enhanced VOC removal efficiency in PLA/CyD and PLA+CyD filters; the FTIR analysis  
 278 confirms that in filters containing CyDs the traces of the interaction between the pollutants and the  
 279 filter are more evident, showing shifted and larger bands, split and sharper peaks. Further studies  
 280 will involve the investigation of the VOC type on the adsorption property, with the simultaneous  
 281 addition of functional composites and the aim of synthesizing such composite from starch-food

282 wastes. The use of CyDs from food wastes in air filtration systems will improve their positive  
283 environmental impact in a circular economy perspective for being used in air filtration applications.  
284

285 **Author Contributions:** Conceptualization, Silvia Palmieri, Mattia Pierpaoli, Luca Riderelli and Sheng  
286 Qi; Data curation, Mattia Pierpaoli, Silvia Palmieri, Luca Riderelli; Formal analysis, Silvia Palmieri,  
287 Luca Riderelli and Maria Letizia Ruello; Investigation, Silvia Palmieri, Luca Riderelli and Sheng Qi;  
288 Methodology, Silvia Palmieri, Mattia Pierpaoli, Luca Riderelli and Sheng Qi; Project administration,  
289 Maria Letizia Ruello; Resources, Sheng Qi and Maria Letizia Ruello; Supervision, Maria Letizia  
290 Ruello; Writing – original draft, Silvia Palmieri and Luca Riderelli; Writing – review & editing, Mattia  
291 Pierpaoli, and Maria Letizia Ruello.

292 **Funding:** This research received no external funding

293 **Acknowledgments:** We would like to thank: Total Corbion PLA for providing the PLA and Dr.  
294 Simona Sabbatini from the SIMAU (Department of Materials, Environmental Sciences and Urban  
295 Planning) for the FTIR measurements.

296 **Conflicts of Interest:** The authors declare no conflict of interest.

## 297 References

- 298 1. Reneker, D.H.; Yarin, A.L.; Zussman, E.; Xu, H. ELECTROSPINNING OF NANOFIBERS  
299 FROM POLYMER SOLUTIONS. *Polymer (Guildf)*. **2007**, doi:10.1016/S0065-2156(06)41002-4.
- 300 2. Krishnan, R.; Sundarrajan, S.; Ramakrishna, S. Green Processing of Nanofibers for  
301 Regenerative Medicine. *Macromol. Mater. Eng.* **2012**, *298*, n/a-n/a,  
302 doi:10.1002/mame.201200323.
- 303 3. Pierpaoli, M.; Ruello, M.L. IAQ: a bibliometric study. **2018**, 1–20.
- 304 4. Yang, F.; Murugan, R.; Wang, S.; Ramakrishna, S. Electrospinning of nano/micro scale poly(l-  
305 lactic acid) aligned fibers and their potential in neural tissue engineering. *Biomaterials* **2005**,  
306 *26*, 2603–2610, doi:10.1016/j.biomaterials.2004.06.051.
- 307 5. Mohammadian, M.; Haghi, A.K. Systematic parameter study for nano-fiber fabrication via  
308 electrospinning process. *Bulg. Chem. Commun.* **2014**, *46*, 545–555,  
309 doi:10.1016/j.polymer.2005.05.068.
- 310 6. Chakraborty, S.; Liao, I.C.; Adler, A.; Leong, K.W. Electrohydrodynamics: A facile technique  
311 to fabricate drug delivery systems. *Adv. Drug Deliv. Rev.* **2009**, *61*, 1043–1054,  
312 doi:10.1016/j.addr.2009.07.013.
- 313 7. You, Y.; Won, S.; Jin, S.; Ho, W. Thermal interfiber bonding of electrospun poly (L-lactic acid  
314 ) nanofibers. **2006**, *60*, 1331–1333, doi:10.1016/j.matlet.2005.11.022.
- 315 8. Park, J.; Lee, I. Controlled release of ketoprofen from electrospun porous polylactic acid (PLA  
316 ) nanofibers. **2011**, 1287–1291, doi:10.1007/s10965-010-9531-0.
- 317 9. Li, Y.; Lim, C.T.; Kotaki, M. Study on structural and mechanical properties of porous PLA  
318 nanofibers electrospun by channel-based electrospinning system. *Polym. (United Kingdom)*  
319 **2015**, *56*, 572–580, doi:10.1016/j.polymer.2014.10.073.
- 320 10. Casasola, R.; Thomas, N.L.; Trybala, A.; Georgiadou, S. Electrospun poly lactic acid (PLA)  
321 fibres: Effect of different solvent systems on fibre morphology and diameter. *Polym. (United*  
322 *Kingdom)* **2014**, *55*, 4728–4737, doi:10.1016/j.polymer.2014.06.032.
- 323 11. Wang, Z.; Zhao, C.; Pan, Z. Porous bead-on-string poly(lactic acid) fibrous membranes for air  
324 filtration. *J. Colloid Interface Sci.* **2015**, *441*, 121–129, doi:10.1016/j.jcis.2014.11.041.
- 325 12. Aulton, M.E.; Taylor, K.M.G. *Tecnologie Farmaceutiche-Progettazione e allestimento dei medicinali*;

- 326 Edra, Ed.; London, 2015; ISBN 9780702042904.
- 327 13. Sliwa, W.; Girek, T. *Cyclodextrins. Properties and Application*; Wiley-VCH, Ed.; 2017; ISBN  
328 9783527339808.
- 329 14. Kayaci, F.; Umu, O.C.O.; Tekinay, T.; Uyar, T. Antibacterial Electrospun Poly(lactic acid)  
330 (PLA) Nanofibrous Webs Incorporating Triclosan/Cyclodextrin Inclusion Complexes. *J. Agric.*  
331 *Food Chem.* **2013**, doi:10.1021/jf400440b.
- 332 15. Arkas, M.; Allabashi, R.; Tsiourvas, D.; Mattausch, E.M.; Perfler, R. Organic/inorganic hybrid  
333 filters based on dendritic and cyclodextrin “nanosponges” for the removal of organic  
334 pollutants from water. *Environ. Sci. Technol.* **2006**, *40*, 2771–2777, doi:10.1021/es052290v.
- 335 16. Favier, I.M.; Baudelet, D.; Fourmentin, S. VOC trapping by new crosslinked cyclodextrin  
336 polymers. In Proceedings of the Journal of Inclusion Phenomena and Macrocyclic Chemistry;  
337 Springer, 2011; Vol. 69, pp. 433–437.
- 338 17. Wen, P.; Zhu, D.H.; Feng, K.; Liu, F.J.; Lou, W.Y.; Li, N.; Zong, M.H.; Wu, H. Fabrication of  
339 electrospun polylactic acid nanofilm incorporating cinnamon essential oil/ $\beta$ -cyclodextrin  
340 inclusion complex for antimicrobial packaging. *Food Chem.* **2016**, *196*, 996–1004,  
341 doi:10.1016/j.foodchem.2015.10.043.
- 342 18. Aytac, Z.; Kusku, S.I.; Durgun, E.; Uyar, T. Encapsulation of gallic acid/cyclodextrin inclusion  
343 complex in electrospun polylactic acid nanofibers: Release behavior and antioxidant activity  
344 of gallic acid. *Mater. Sci. Eng. C* **2016**, *63*, 231–239, doi:10.1016/j.msec.2016.02.063.
- 345 19. Loftsson, T.; Duchêne, D. Cyclodextrins and their pharmaceutical applications. *Int. J. Pharm.*  
346 **2007**, *329*, 1–11, doi:10.1016/j.ijpharm.2006.10.044.
- 347 20. Butterfield, M.T.; Agbaria, R.A.; Warner, I.M. Extraction of volatile PAHs from air by use of  
348 solid cyclodextrin. *Anal. Chem.* **1996**, *68*, 1187–1190, doi:10.1021/ac9510144.
- 349 21. Crini, G.; Peindy, H.N.; Gimbert, F.; Robert, C. Removal of C.I. Basic Green 4 (Malachite  
350 Green) from aqueous solutions by adsorption using cyclodextrin-based adsorbent: Kinetic  
351 and equilibrium studies. *Sep. Purif. Technol.* **2007**, *53*, 97–110, doi:10.1016/j.seppur.2006.06.018.
- 352 22. Alsbaiee, A.; Smith, B.J.; Xiao, L.; Ling, Y.; Helbling, D.E.; Dichtel, W.R. Rapid removal of  
353 organic micropollutants from water by a porous  $\beta$ -cyclodextrin polymer. *Nature* **2016**, *529*,  
354 190–194, doi:10.1038/nature16185.
- 355 23. Pierpaoli, M.; Riderelli, L.; Palmieri, S.; Fava, G.; Ruello, M.L. Transparent electrospun PLA-  
356 nanofibers on 3D-printed honeycomb for a high-efficient air filtration . **2017**, 2–3.
- 357 24. Medhurst, L.J. FTIR Determination of Pollutants in Automobile Exhaust : An Environmental  
358 Chemistry Experiment Comparing Cold-Start and Warm-Engine Conditions. **2005**, 82.
- 359 25. Qin, X.; Wang, S. Filtration Properties of Electrospinning Nanofibers. **2006**,  
360 doi:10.1002/app.24361.
- 361 26. Uyar, T.; Havelund, R.; Hacaloglu, J.; Besenbacher, K.F.; Kingshott, P. Cyclodextrins :  
362 Comparison of Molecular Filter Performance. *ACS Nano* **2010**, *4*, 5121–5130.
- 363 27. A Novel Hierarchical Structured Poly(lactic acid)/Titania Fibrous Membrane with Excellent  
364 Antibacterial Activity and Air Filtration Performance., doi:10.1155/2016/6272983.
- 365 28. Li, H.; Wang, Z.; Zhang, H.; Pan, Z. Nanoporous PLA/(Chitosan Nanoparticle) Composite  
366 Fibrous Membranes with Excellent Air Filtration and Antibacterial Performance. *Polymers*  
367 *(Basel)*. **2018**, *10*, 1085, doi:10.3390/polym10101085.
- 368 29. Zhang, Q.; Li, Q.; Young, T.M.; Harper, D.P.; Wang, S. A Novel Method for Fabricating an

- 369 Electrospun Poly(Vinyl Alcohol)/Cellulose Nanocrystals Composite Nanofibrous Filter with  
370 Low Air Resistance for High-Efficiency Filtration of Particulate Matter. *ACS Sustain. Chem.*  
371 *Eng.* **2019**, *7*, 8706–8714, doi:10.1021/acssuschemeng.9b00605.
- 372 30. Wang, Z.; Pan, Z. Preparation of hierarchical structured nano-sized/porous poly(lactic acid)  
373 composite fibrous membranes for air filtration. *Appl. Surf. Sci.* **2015**, *356*, 1168–1179,  
374 doi:10.1016/j.apsusc.2015.08.211.
- 375 31. Huang, J.J.; Tian, Y.; Wang, R.; Tian, M.; Liao, Y. Fabrication of bead-on-string  
376 polyacrylonitrile nanofibrous air filters with superior filtration efficiency and ultralow  
377 pressure drop. *Sep. Purif. Technol.* **2020**, *237*, 116377, doi:10.1016/j.seppur.2019.116377.
- 378 32. Pierpaoli, M.; Zheng, X.; Bondarenko, V.; Fava, G.; Ruello, M.L. Paving the Path to A  
379 Sustainable and Efficient SiO<sub>2</sub> / TiO<sub>2</sub> Photocatalytic Composite. **2019**, 1–14.
- 380



© 2020 by the authors. Submitted for possible open access publication under the terms and conditions of the Creative Commons Attribution (CC BY) license (<http://creativecommons.org/licenses/by/4.0/>).